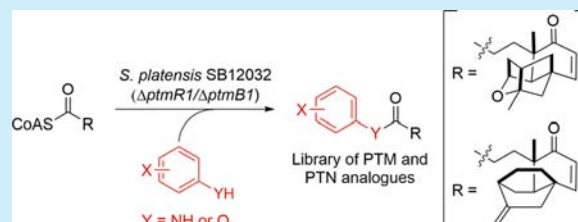


A Mutasynthetic Library of Platensimycin and Platencin Analogues

Liao-Bin Dong,^{†,||} Jeffrey D. Rudolf,^{†,||} and Ben Shen^{*,†,‡,§}[†]Department of Chemistry, [‡]Department of Molecular Therapeutics, and [§]Natural Products Library Initiative at The Scripps Research Institute, The Scripps Research Institute, Jupiter, Florida 33458, United States

S Supporting Information

ABSTRACT: Inactivation of *ptmB1*, *ptmB2*, *ptmT2*, or *ptmC* in *Streptomyces platensis* SB12029, a platensimycin (PTM) and platencin (PTN) overproducer, revealed that PTM and PTN biosynthesis features two distinct moieties that are individually constructed and convergently coupled to afford PTM and PTN. A focused library of PTM and PTN analogues was generated by mutasynthesis in the Δ *ptmB1* mutant *S. platensis* SB12032. Of the 34 aryl variants tested, 18 were incorporated with high titers.



Platensimycin (PTM, **1m**) and platencin (PTN, **1n**) are selective and potent bacterial and mammalian fatty acid synthase inhibitors. They are effective against a broad range of bacterial pathogens, including methicillin-resistant *Staphylococcus aureus* (MRSA), vancomycin-resistant *Enterococci* (VRE), and *Mycobacterium tuberculosis*.¹ PTM and PTN have also demonstrated efficacy in animal models as a new class of antibacterial and antidiabetic drug leads.² However, it is imperative to generate PTM and PTN analogues to improve their poor pharmacokinetics, as they had to be continuously infused into mice in order to achieve antibiotic efficacy *in vivo*.^{1b}

PTM and PTN are comprised of two distinct motifs, a highly modified diterpene-derived aliphatic cage (ketolide) and a 3-amino-2,4-dihydroxybenzoic acid (ADHBA), linked together by an amide bond (Figure 1A).³ We previously cloned and sequenced the biosynthetic gene clusters encoding PTM and PTN production from the PTM–PTN dual producer *Streptomyces platensis* MA7327 and the PTN producer *S. platensis* MA7339, respectively (Figure S1).⁴ The high similarities between the *ptm* and *ptn* gene clusters suggested that a conserved set of enzymes was able to process two different ketolide scaffolds into PTM and PTN. We initially proposed a convergent biosynthetic pathway where (i) one set of enzymes biosynthesizes the ADHBA moiety, (ii) another set of enzymes biosynthesizes the *ent*-kaurene and *ent*-atiserene scaffolds and processes them into the penultimate intermediates platensicyl- and platencinyl-CoA, and (iii) a final coupling reaction links ADHBA with platensicyl- or platencinyl-CoA to form PTM and PTN, respectively (Figure 1B–D).⁴

We recently discovered six additional dual PTM–PTN-producing *S. platensis* strains.⁵ By inactivating the negative transcriptional regulator *ptmR1* in *S. platensis* CB00739, we established a model strain, SB12029, for the study of PTM and PTN.⁶ The dramatic overproduction of PTM and PTN (up to 300 mg L^{−1}), along with the ability to genetically manipulate SB12029, gave us outstanding opportunities to carry out functional characterization of the PTM and PTN biosynthetic pathway and to explore the promiscuity of the tailoring enzymes

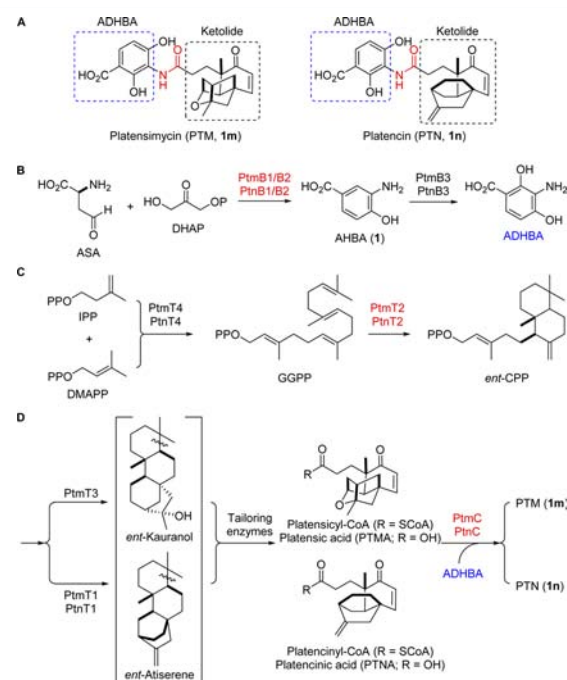


Figure 1. Convergent biosynthesis for PTM and PTN. (A) Structures of PTM (**1m**) and PTN (**1n**) highlighting the ADHBA and diterpene-derived ketolide moieties linked by an amide bond. (B) Biosynthesis of ADHBA, (C) *ent*-copalyl diphosphate (*ent*-CPP), and (D) the ketolides of PTM and PTN, which are coupled to ADHBA in the final step. *PtmB1*/*PtnB1*, *PtmB2*/*PtnB2*, *PtmT2*/*PtnT2*, and *PtmC*/*PtnC* are highlighted in red.

found within the biosynthetic machinery to generate PTM and PTN structural diversity.

Herein, we first report three production phenotypes that support the convergent nature of the PTM and PTN

Received: July 29, 2016

Published: September 6, 2016

biosynthetic pathways. Deletion of key genes involved in the biosynthesis of the ADHBA (*ptmB1* or *ptmB2*), ketolide moieties (*ptmT2*), or the linkage between these two moieties (*ptnC*), within the PTM–PTN-overproducing strain SB12029 resulted in mutant strains that all abolished PTM and PTN production but accumulated ADHBA only (Δ *ptmT2*), ketolides only (Δ *ptmB1* or Δ *ptmB2*), or both (Δ *ptmC*), respectively, in high titers. We then utilized SB12032, which was unable to biosynthesize 3-amino-4-hydroxybenzoic acid (AHBA, **1**), the immediate precursor of ADHBA, to test the capability of the PTM and PTN biosynthetic machinery to couple unnatural benzoate analogues, in vivo, to the ketolide moieties for the preparation of a focused PTM and PTN library.

The structures of PTM and PTN both possess an ADHBA moiety, which is biosynthetically constructed by PtmB1/PtnB1, PtmB2/PtnB2, and PtmB3/PtnB3 (Figure 1B). PtmB1/PtnB1 and PtmB2/PtnB2 are proposed to catalyze the formation of **1** from aspartate semialdehyde (ASA) and dihydroxyacetone phosphate (DHAP).^{4,7} PtmB3/PtnB3 then regiospecifically hydroxylates the C-2 position of **1** to afford ADHBA for both PTM and PTN biosynthesis.⁸ In an effort to construct an AHBA-blocked mutant in the engineered PTM and PTN overproducer SB12029 (i.e., Δ *ptmR1*), we used λ RED-mediated PCR-targeting mutagenesis⁹ [see the Supporting Information for experimental details and Tables S1–S3] to inactivate *ptmB1* or *ptmB2* in SB12029 to afford the double mutants SB12032 (i.e., Δ *ptmR1*/ Δ *ptmB1*) and SB12033 (i.e., Δ *ptmR1*/ Δ *ptmB2*), respectively (Figures S2 and S3). When cultured under previously described conditions for PTM and PTN production, as well as the sulfur-containing analogues PTM S1 and PTN S1, in SB12029 (Figure 2B, panel I),¹⁰ analysis of the crude extract of

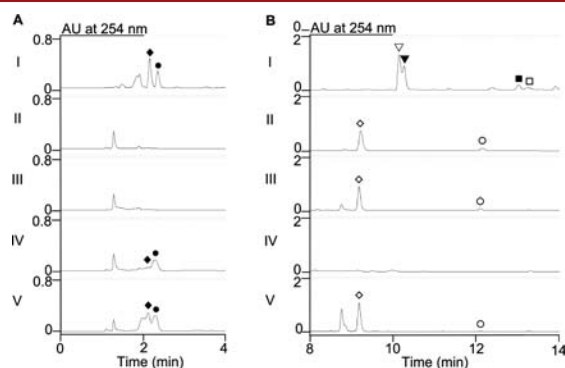


Figure 2. LC–MS analysis of *S. platensis* recombinant strains. Aqueous layers (A) or crude extracts (B) of each strain were analyzed using UV detection at λ_{254} : (I) SB12029 (CB00739 Δ *ptmR1*); (II) SB12032 (SB12029 Δ *ptmB1*); (III) SB12033 (SB12029 Δ *ptmB2*); (IV) SB12034 (SB12029 Δ *ptmT2*); (V) SB12035 (SB12029 Δ *ptmC*). Key: ●, AHBA; ◆, ADHBA; ◇, PTMA; ○, PTNA; ▽, PTM S1; ▼, PTM; ■, PTN; □, PTN S1.

SB12032 and SB12033 showed that the PTM and PTN production was completely abolished; only platensic (PTMA) and platencinic (PTNA) acids, the hydrolyzed products of platensicyl- and platencinyl-CoA, respectively (Figure 1D), were detected (Figure 2B, panels II and III). Neither **1** nor ADHBA was detected in the aqueous layers of SB12032 or SB12033 (Figure 2A, panels II and III) after extraction (S1). Although the PTNA titers were low in both SB12032 (4.7 ± 0.8 mg L^{−1}) and SB12033 (3.2 ± 0.5 mg L^{−1}), the PTMA titers were high, with 147 ± 17 mg L^{−1} in SB12032 and 145 ± 9 mg L^{−1} in SB12033,

respectively. Both strains were chemically complemented upon addition of **1** to the fermentation medium, restoring PTM and PTN production and yielding small amounts of 3'-dehydroxy-PTM and -PTN (Figure S6).

Biosynthesis of the diterpenoid moieties begins with geranylgeranyl diphosphate (GGPP) synthase (PtmT4/PtnT4) followed by *ent*-CPP synthase (PtmT2/PtnT2) to form *ent*-CPP (Figure 1C).⁴ Two dedicated diterpene synthases, PtmT3 and PtmT1/PtnT1, then partition PTM and PTN biosynthesis by catalyzing the cyclization of *ent*-CPP into *ent*-kauranol and *ent*-atiserene, respectively (Figure 1D).^{4,11} A group of tailoring enzymes, which must inherently possess relaxed substrate specificity, processes both diterpene scaffolds to furnish the final ketolide moieties PTMA and PTNA (Figure 1D). Inactivation of *ptmT2* therefore should abolish the production of all *ent*-CPP-derived diterpenes (i.e., PTMA and PTNA); production of **1** and ADHBA, however, should remain unaffected. Inactivation of *ptmT2* in SB12029 afforded SB12034 (i.e., Δ *ptmR1*/ Δ *ptmT2*, Figure S4), fermentation of which indeed yielded neither PTM, PTN, PTMA, PTNA, nor any intermediates or congeners previously isolated from mutants or wild-type strains (Figure 2B, IV); however, both **1** and ADHBA were produced (Figure 2A, panel IV). When SB12034 was chemically complemented with (11S,16S)-*ent*-kauran-11,16-epoxy-19-oic acid,¹² a PTMA intermediate isolated from SB12030,⁶ PTM production was restored (Figure S6).

PtmC/PtnC belongs to the arylamine *N*-acetyltransferases superfamily¹³ and was proposed to catalyze the final coupling step in PTM and PTN biosynthesis.⁴ We inactivated *ptmC* in SB12029 to afford SB12035 (i.e., Δ *ptmR1*/ Δ *ptmC*, Figure S5). As expected, fermentation of SB12035 revealed the production of **1** and ADHBA (Figure 2A, panel V), as well as PTMA and PTNA (Figure 2B, panel V). As the ketolide and ADHBA moieties were both present, but the coupled final products PTM and PTN were not detected, PtmC is supported as the amide synthase responsible for the final coupling step in the PTM and PTN biosynthesis.

Inspired by the findings that PTM and PTN are biosynthesized in a convergent manner, we set out to produce a focused PTM and PTN library, with varying ADHBA moieties, by a mutasynthesis strategy (Table 1). Thirty-four commercially available aryl variants (Figure S7) were selected to test the capability of the PTM and PTN biosynthetic machinery to couple them to the ketolide moieties in vivo. We supplemented SB12032 with 0.2 mg mL^{−1} of each aryl variant and analyzed the crude extracts of each of the fermentations by LC–MS to determine whether the coupling was successful. For clarity, each aryl variant is numbered 1–34, and coupled products are numbered 1–34 with an “m” or “n” denotation according to which ketolide scaffold, PTMA or PTNA, was coupled (e.g., **1m** and **1n** for PTM and PTN, respectively) (Table 1).

Of the 34 aryl variants tested, 18 were successfully coupled to the ketolides (Table 1 and Figure S8). The aryl variants tested could be divided into six categories: 3-aminobenzoic acids (*meta*), 4-aminobenzoic acids (*para*), 2-aminobenzoic acids (*ortho*), aminomethyl- or hydroxymethylbenzoic acids (both *meta* and *para*), heteroarylamines, and arylamines. Surprisingly, members (1–3, 6–8, 13, 17–20, 24, 27, 29, and 31–34) of each of the six categories were successfully incorporated, indicating that the biosynthetic machinery of PTM and PTN, and specifically PtmC/PtnC, is extremely flexible in regard to its aryl variant substrate. The varying production titers of the coupled products, together with the inability to incorporate the

Table 1. Mutasynthesis with Aryl Variants in SB12032

nr. ^a	compound	product ^b	yield ^c
3-, 4-, or 2-aminobenzoic acids			
1			+++
2			+++
3			+++ (115)
6			+++ (67)
7			+++ (168)
8			+++ (22)
13			++ (33)
amino/hydroxymethylbenzoic acids			
17			+ (3.5)
18			+
19			+ (4.2)
20			+
heteroarylamines			
24			++ (14)
arylamines			
27			++ (14)
			+ (3.0)
29			+
31			+
32			++ (23)
33			+
34			++ (21)

^aSee Figure S7 for a full list of tested compounds. ^bR = PTM or PTN ketolides; see Figure S9 for full structures; see Tables S4–S9 and Figures S11–S34 for NMR data. ^cQualitative titers based on LC–MS analysis (+, ++, or +++); titers (mg L^{−1}) are given in parentheses for each isolated PTM product.

other 16 aryl variants tested, reveal insights into the substrate preference of the coupling reaction.

Considering ADHBA contains a *meta* amino group, it was unsurprising that 3-aminobenzoic acids (1–3) were readily coupled to the ketolides (Table 1). As an example, when 5-amino-2-fluorobenzoic acid (3) was added to a fermentation of SB12032, two new peaks were detected in the LC–MS

chromatogram (Figure S8), the *m/z* values of which were consistent with the PTM- and PTN-coupled products of 3m and 3n, respectively. The high ketolide titers of SB12032 and excellent incorporation of 3 facilitated the isolation of 3m (115 mg L^{−1}), the structure of which was subsequently confirmed by 1D and 2D NMR spectroscopy (SI). Not all 3-aminobenzoic acids, however, were incorporated into PTM and PTN derivatives. When the 4-OH in AHBA was substituted by 4-OCH₃ (4) or 4-Cl (5), no coupled products were detected.

4-Aminobenzoic acids 6–8 were also efficiently incorporated into PTM and PTN analogues. Compounds 6m (67 mg L^{−1}) and 7m (168 mg L^{−1}) were isolated, and their structures were confirmed by 1D and 2D NMR spectroscopy (SI). Since both 3-amino- and 4-aminobenzoic acids were successfully incorporated with high efficiencies, we tested the preference of *meta* and *para* amino substitutions by feeding 3,4-diaminobenzoic acid (8) to SB12032. LC–MS analysis showed high levels of 8m-a and 8n-a (Figure S8). Two minor products (8m-b and 8n-b) were additionally detected, the *m/z* of which were 18 Da less than those of 8m-a and 8n-b, respectively, suggesting they may be dehydrated analogues. Unfortunately, 8m-a was extremely unstable during purification and spontaneously transformed into 8m-b. The structure of 8m-b, possessing a unique benzimidazole moiety, was determined by a combination of HRMS and 1D and 2D NMR spectroscopy and confirmed that 8m-b is likely the nonenzymatic dehydration product of 8m-a (SI). Due to the interconversion of the benzimidazole group, we were unable to establish whether the 3- or 4-amide was the dominant coupled product (Figure S10).

Of the five 2-aminobenzoic acids (9–13) tested, only 2-amino-3-hydroxybenzoic acid (13) was incorporated (Figure S8). Analogue 13m (33 mg L^{−1}) was subsequently isolated, and its structure was fully characterized (SI). Consistent with the inability to incorporate 2-aminobenzoic acids, 13m did not contain an amide linkage. Instead, it contained an ester linkage at 3-OH and is the first PTM or PTN analogue with an ester linkage. Encouraged by the ability of the biosynthetic machinery to form ester linkages, three additional 3-hydroxybenzoic acids (14–16) were tested. LC–MS analysis revealed, however, that none of these analogues was converted into PTM or PTN analogues by SB12032. However, two (hydroxymethyl)benzoic acids (18, 20) and two aminomethylbenzoic acids (17, 19), with either *meta* and *para* substitutions, were each successfully incorporated with comparable titers (SI).

Six heteroarylamines, including a thiazole (21), four pyridines (22–25), and a pyrimidine (26), were added to a culture of SB12032. Only 5-aminonicotinic acid (24) was successfully incorporated with moderate efficiency and led to the isolation of 24m (14 mg L^{−1}, SI), the first pyridine-derived PTM analogue.

Finally, we investigated whether the carboxylic acid group is compulsory for the coupling reaction. When SB12032 was supplemented with arylamines containing nitro (27), sulfonic acid (29), chloro (31), hydroxyl (32), or methoxyl (33) groups in place of the carboxylic acid, coupled products were detected (Figure S8). Again, nitro- and sulfonic acid-containing analogues with 4-OCH₃ groups, 28 and 30, failed to be incorporated. As it appeared that the carboxylic acid was not essential for coupling, we hypothesized that aniline (34) might also be incorporated. This was indeed confirmed by the isolation of 34m (21 mg L^{−1}, SI) after feeding 34 to a fermentation culture of SB12032.

We initially envisioned that if we only inactivated *ptmB1* or *ptmB2*, *PtmB3* may hydroxylate 1 or 2–34 should it be promiscuous. However, only two compounds, 1 and 27,

appeared to be hydroxylated, leading to additional PTM and PTN analogues. Not surprisingly, **1**, the native substrate of PtmB3, was hydroxylated to yield ADHBA. Addition of 3-nitroaniline (**27**) yielded the expected analogue containing the 3-nitroaniline moiety (**27m-a**, 14 mg L⁻¹) as well as an analogue containing an additional hydroxyl group on the aniline ring at C-6 (**27m-b**, 3 mg L⁻¹).

Our efforts to construct a focused library of PTM and PTN analogues also revealed key insights into the permissibility and limitations of the coupling reaction. Overall, this *in vivo* study supports PtmC as an amide synthase with extreme flexibility for its aryl variant substrate as 18 of the 34 tested aryl variants were incorporated in the biosynthetic pathway and led to the generation of more than 30 PTM and PTN analogues. Three mechanistic implications regarding the coupling reaction were discovered: (i) the benzoic acid is not compulsory; (ii) amide and ester linkages can be formed from *meta* and *para* positions, but not *ortho*; and (iii) large functional groups *ortho* to the amine prevent coupling. Further biochemical evidence is needed, however, to fully understand the substrate and chemical specificity of the coupling reaction.

Each of the PTM analogues isolated (**3m**, **6m**, **7m**, **8m-b**, **13m**, **17m**, **19m**, **24m**, **27m-a**, **27m-b**, **32m**, and **34m**) was tested for antibacterial activity against *Micrococcus luteus* ATCC 9431 and *Staphylococcus aureus* ATCC 25923 (SI). Although none of the isolated PTM analogues showed antibacterial activity up to 80 µg per disk with PTM, at 5 µg per disk, as a positive control, these findings provided additional experimental data supporting the current structure–activity relationship (SAR) for PTM.^{10,14}

In summary, we reported three distinct phenotypes in the PTM and PTN overproducer *S. platensis* SB12029 by the inactivation of key genes involved in the biosynthesis of the ADHBA (Δ ptmB1 or Δ ptmB2), ketolide moieties (Δ ptmT2), or the linkage (Δ ptmC) between these two moieties. The convergent nature and flexibility of the PTM and PTN biosynthetic pathways facilitated construction of a focused library of analogues via mutasynthesis. Although none of the PTM analogues isolated in this study retained the antibacterial activity of PTM, they provide important experimental evidence supporting the current SAR for PTM. Importantly, this study sets the stage to explore additional aryl variants and investigate the feasibility of preparing designer PTM and PTN analogues by a mutasynthetic strategy. Finally, after successful generation of PTM and PTN analogues with modified aminobenzoic acids, one could easily envisage generating structural diversity in the diterpene-derived ketolide moiety. The high and facile production of PTM and PTN analogues by mutasynthesis encourages the continued development of novel unnatural products that will focus on understanding the SAR of PTM and PTN and addressing the poor pharmacokinetics of these natural product drug leads. A focused library of PTM and PTN analogues will also provide opportunities to explore the privileged scaffolds of PTM and PTN for other targets of biological significance.

■ ASSOCIATED CONTENT

Supporting Information

The Supporting Information is available free of charge on the ACS Publications website at DOI: 10.1021/acs.orglett.6b02248.

Complete experimental procedures, Tables S1–S9, and Figures S1–S34 (PDF)

■ AUTHOR INFORMATION

Corresponding Author

*E-mail: shenb@scripps.edu.

Author Contributions

^{||}L.-B.D. and J.D.R. contributed equally to this work.

Notes

The authors declare no competing financial interest.

■ ACKNOWLEDGMENTS

We thank the John Innes Center, Norwich, UK, for providing the REDIRECT Technology kit. This work is supported in part by the National Institutes of Health Grant No. GM114353 (B.S.). J.D.R. is supported in part by an Arnold O. Beckman Postdoctoral Fellowship.

■ REFERENCES

- (1) (a) Brown, A. K.; Taylor, R. C.; Bhatt, A.; Fütterer, K.; Besra, G. S. *PLoS One* **2009**, *4*, e6306. (b) Wang, J.; Kodali, S.; Lee, S. H.; Galgoci, A.; Painter, R.; Dorso, K.; Racine, F.; Motyl, M.; Hernandez, L.; Tinney, E.; et al. *Proc. Natl. Acad. Sci. U. S. A.* **2007**, *104*, 7612–7616. (c) Wang, J.; Soisson, S. M.; Young, K.; Shoop, W.; Kodali, S.; Galgoci, A.; Painter, R.; Parthasarathy, G.; Tang, Y. S.; Cummings, R.; et al. *Nature* **2006**, *441*, 358–361.
- (2) Wu, M.; Singh, S. B.; Wang, J.; Chung, C. C.; Salituro, G.; Karanam, B. V.; Lee, S. H.; Powles, M.; Ellsworth, K. P.; Lassman, M. E.; et al. *Proc. Natl. Acad. Sci. U. S. A.* **2011**, *108*, 5378–5383.
- (3) (a) Jayasuriya, H.; Herath, K. B.; Zhang, C.; Zink, D. L.; Basilio, A.; Genilloud, O.; Diez, M. T.; Vicente, F.; Gonzalez, I.; Salazar, O.; et al. *Angew. Chem., Int. Ed.* **2007**, *46*, 4684–4688. (b) Singh, S. B.; Jayasuriya, H.; Ondeyka, J. G.; Herath, K. B.; Zhang, C.; Zink, D. L.; Tsou, N. N.; Ball, R. G.; Basilio, A.; Genilloud, O.; et al. *J. Am. Chem. Soc.* **2006**, *128*, 11916–11920.
- (4) (a) Smanski, M. J.; Yu, Z.; Casper, J.; Lin, S.; Peterson, R. M.; Chen, Y.; Wendt-Pienkowski, E.; Rajske, S. R.; Shen, B. *Proc. Natl. Acad. Sci. U. S. A.* **2011**, *108*, 13498–13503. (b) Rudolf, J. D.; Dong, L.-B.; Cao, H.; Hatzos-Skintges, C.; Osipiuk, J.; Endres, M.; Chang, C.-Y.; Ma, M.; Babnigg, G.; Joachimiak, A.; et al. *J. Am. Chem. Soc.* **2016**, *138*, 10905–10915.
- (5) Hindra; Huang, T.; Yang, D.; Rudolf, J. D.; Xie, P.; Xie, G.; Teng, Q.; Lohman, J. R.; Zhu, X.; Huang, Y.; et al. *J. Nat. Prod.* **2014**, *77*, 2296–2303.
- (6) Rudolf, J. D.; Dong, L.-B.; Huang, T.; Shen, B. *Mol. Biosyst.* **2015**, *11*, 2717–2726.
- (7) Suzuki, H.; Ohnishi, Y.; Furusho, Y.; Sakuda, S.; Horinouchi, S. *J. Biol. Chem.* **2006**, *281*, 36944–36951.
- (8) (a) Waldman, A. J.; Pechersky, Y.; Wang, P.; Wang, J. X.; Balskus, E. P. *ChemBioChem* **2015**, *16*, 2172–2175. (b) Sugai, Y.; Katsuyama, Y.; Ohnishi, Y. *Nat. Chem. Biol.* **2015**, *12*, 73–75.
- (9) Gust, B.; Challis, G. L.; Fowler, K.; Kieser, T.; Chater, K. F. *Proc. Natl. Acad. Sci. U. S. A.* **2003**, *100*, 1541–1546.
- (10) Dong, L.-B.; Rudolf, J. D.; Shen, B. *Bioorg. Med. Chem.* **2016**, DOI: 10.1016/j.bmc.2016.04.026.
- (11) Smanski, M. J.; Peterson, R. M.; Huang, S.-X.; Shen, B. *Curr. Opin. Chem. Biol.* **2012**, *16*, 132–141.
- (12) Murakami, T.; Iida, H.; Tanaka, N.; Saiki, Y.; Chen, C.-M.; Iitaka, Y. *Chem. Pharm. Bull.* **1981**, *29*, 657–662.
- (13) Sim, E.; Sandy, J.; Evangelopoulos, D.; Fullam, E.; Bhakta, S.; Westwood, I.; Krylova, A.; Lack, N.; Noble, M. *Curr. Drug Metab.* **2008**, *9*, 510–519.
- (14) Nicolaou, K.; Stepan, A. F.; Lister, T.; Li, A.; Montero, A.; Tria, G. S.; Turner, C. I.; Tang, Y.; Wang, J.; Denton, R. M.; et al. *J. Am. Chem. Soc.* **2008**, *130*, 13110–13119.